

Population transfer driven by far-off-resonant fields

Z. C. Shi,^{1,2} W. Wang,² and X. X. Yi^{2,*}

¹Department of Physics, Fuzhou University, Fuzhou 350002, China

²Center for Quantum Sciences and School of Physics, Northeast Normal University, Changchun 130024, China

[*yixx@nenu.edu.cn](mailto:yixx@nenu.edu.cn)

Abstract: For a two-level system, it is believed that a far-off-resonant driving can not help coherent population transfer between two states. In this work, we propose a scheme to implement the coherent transfer with far-off-resonant driving. The scheme works well with both constant driving and Gaussian driving. The total time to finish population transfer is also minimized by optimizing the detuning and coupling constants. We find that the scheme is sensitive to spontaneous emission much more than dephasing. It might find potential applications in X-ray quantum optics and population transfer in Rydberg atoms as well.

© 2016 Optical Society of America

OCIS codes: (270.0270) Quantum optics; (270.5580) Quantum electrodynamics.

References and links

1. M. O. Scully and M. S. Zubairy, *Quantum Optics* (Cambridge University, 1997).
2. M. Nielsen and I. Chuang, *Quantum Computation and Quantum Information* (Cambridge University, 2010).
3. M. Saffman, T. G. Walker, and K. Mølmer, "Quantum information with Rydberg atoms," *Rev. Mod. Phys.* **82**, 2313 (2010).
4. H. Schempp, G. Günter, S. Wüster, M. Weidemüller, and S. Whitlock, "Correlated exciton transport in Rydberg-dressed-atom spin chains," *Phys. Rev. Lett.* **115**, 093002 (2015).
5. D. Barredo, H. Labuhn, S. Ravets, T. Lahaye, A. Browaeys, and C. S. Adams, "Coherent excitation transfer in a spin chain of three Rydberg atoms," *Phys. Rev. Lett.* **114**, 113002 (2015).
6. P. Walker and G. Dracoulis, "Energy traps in atomic nuclei," *Nature* **399**, 35–40 (1999).
7. K. W. D. Ledingham, P. McKenna, and R. P. Singhal, "Applications for nuclear phenomena generated by ultra-intense lasers," *Science* **300**, 1107–1111 (2003).
8. A. Aprahamian and Y. Sun, "Nuclear physics: Long live isomer research," *Nature Physics* **1**, 81–82 (2005).
9. A. Pálffy, J. Evers, and C. H. Keitel, "Isomer triggering via nuclear excitation by electron capture," *Phys. Rev. Lett.* **99**, 172502 (2007).
10. K. Bergmann, H. Theuer, and B. W. Shore, "Coherent population transfer among quantum states of atoms and molecules," *Rev. Mod. Phys.* **70**, 1003 (1998).
11. T. J. Bürvenich, J. Evers, and C. H. Keitel, "Nuclear quantum optics with X-ray laser pulses," *Phys. Rev. Lett.* **96**, 142501 (2006).
12. M. Altarelli, R. Brinkmann, M. Chergui, W. Decking, B. Dobson, S. Düsterer, G. Grübel, W. Graeff, H. Graafsma, J. Hajdu, J. Marangos, J. Pflüger, H. Redlin, D. Riley, I. Robinson, J. Rossbach, A. Schwarz, K. Tiedtke, T. Tschentscher, I. Vartanians, H. Wabnitz, H. Weise, R. Wichmann, K. Witte, A. Wolf, M. Wulff, and M. Yurkov, "The European X-Ray Free-Electron Laser Technical design report," (DESY, 2007).
13. A. Pálffy, J. Evers, and C. H. Keitel, "Electric-dipole-forbidden nuclear transitions driven by super-intense laser fields," *Phys. Rev. C* **77**, 044602 (2008).
14. D. G. Baranov, A. P. Vinogradov, and A. A. Lisiansky, "Abrupt Rabi oscillations in a superoscillating electric field," *Opt. Lett.* **39**, 6316–6319 (2014).
15. R. Ber and M. Schwartz, "Unusual transitions made possible by superoscillations," arXiv:1502.01406 (2015).
16. A. Kempf and A. Prain, "Driving quantum systems with superoscillations," arXiv:1510.04353 (2015).
17. M. S. P. Eastham, *The Spectral Theory of Periodic Differential Equations* (Scottish Academic, 1973).

18. H. P. Breuer and F. Petruccione, *The Theory of Open Quantum System* (Oxford University, 2002).
19. I. I. Rabi, "On the process of space quantization," *Phys. Rev.* **49**, 324 (1936).
20. I. I. Rabi, "Space quantization in a gyrating magnetic field," *Phys. Rev.* **51**, 652 (1937).
21. E. Solano, "Viewpoint: The dialogue between quantum light and matter," *Physics* **4**, 68 (2011).
22. V. V. Albert, "Quantum Rabi model for N-state atoms," *Phys. Rev. Lett.* **108**, 180401 (2012).
23. M. J. Hwang, R. Puebla, and M. B. Plenio, "Quantum phase transition and universal dynamics in the Rabi model," *Phys. Rev. Lett.* **115**, 180404 (2015).
24. D. Braak, "Integrability of the Rabi model," *Phys. Rev. Lett.* **107**, 100401 (2011).
25. Q. H. Chen, C. Wang, S. He, T. Liu, and K. L. Wang, "Exact solvability of the quantum Rabi model using Bogoliubov operators," *Phys. Rev. A* **86**, 023822 (2012).
26. E. T. Jaynes and F. W. Cummings, "Comparison of quantum and semiclassical radiation theories with application to the beam maser," *Proc. IEEE* **51**, 89–109 (1963).
27. S. N. Shevchenko, S. Ashhab, and F. Nori, "Landau-Zener-Stückelberg interferometry," *Phys. Rep.* **492**, 1–30 (2010).
28. P. Huang, J. Zhou, F. Fang, X. Kong, X. Xu, C. Ju, and J. Du, "Landau-Zener-Stückelberg interferometry of a single electronic spin in a noisy environment," *Phys. Rev. X* **1**, 011003 (2011).
29. A. Ferrón, Daniel Domínguez and M. Sánchez, "Tailoring population inversion in Landau-Zener-Stückelberg interferometry of flux qubits," *Phys. Rev. Lett.* **109**, 237005 (2012).
30. G. Cao, H. O. Li, T. Tu, L. Wang, C. Zhou, M. Xiao, G. C. Guo, H. W. Jiang, and G. P. Guo, "Ultrafast universal quantum control of a quantum-dot charge qubit using Landau-Zener-Stückelberg interference," *Nat. Commun.* **4**, 1401 (2013).
31. E. Dupont-Ferrier, B. Roche, B. Voisin, X. Jehl, R. Wacquez, M. Vinet, M. Sanquer, and S. De Franceschi, "Coherent coupling of two dopants in a Silicon nanowire probed by Landau-Zener-Stückelberg interferometry," *Phys. Rev. Lett.* **110**, 136802 (2013).
32. A. Izmailkov, M. Grajcar, E. Il'ichev, N. Oukhanski, T. Wagner, H. G. Meyer, W. Krech, M. H. S. Amin, A. Maassen van den Brink, and A. M. Zagoskin, "Observation of macroscopic Landau-Zener transitions in a superconducting device," *Europhys. Lett.* **65**, 844 (2004).
33. W. D. Oliver, Y. Yu, J. C. Lee, K. K. Berggren, L. S. Levitov, and T. P. Orlando, "Mach-Zehnder interferometry in a strongly driven superconducting qubit," *Science* **310**, 1653–1657 (2005).
34. M. Sillanpää, T. Lehtinen, A. Paila, Y. Makhlin, and P. Hakonen, "Continuous-time monitoring of Landau-Zener interference in a Cooper-pair box," *Phys. Rev. Lett.* **96**, 187002 (2006).
35. A. Izmailkov, S. H. W. van der Ploeg, S. N. Shevchenko, M. Grajcar, E. Il'ichev, U. Hübner, A. N. Omelyanchouk, and H. G. Meyer, "Consistency of ground state and spectroscopic measurements on flux qubits," *Phys. Rev. Lett.* **101**, 017003 (2008).
36. M. D. LaHaye, J. Suh, P. M. Echternach, K. C. Schwab, and M. L. Roukes, "Nanomechanical measurements of a superconducting qubit," *Nature* **459**, 960–964 (2009).
37. J. Johansson, M. H. S. Amin, A. J. Berkley, P. Bunyk, V. Choi, R. Harris, M. W. Johnson, T. M. Lanting, Seth Lloyd, and G. Rose, "Landau-Zener transitions in a superconducting flux qubit," *Phys. Rev. B* **80**, 012507 (2009).
38. M. P. Silveri, K. S. Kumar, J. Tuorila, J. Li, A. Vepsäläinen, E. V. Thuneberg, and G. S. Paraoanu, "Stückelberg interference in a superconducting qubit under periodic latching modulation," *New J. Phys.* **17**, 043058 (2015).
39. N. Thaicharoen, A. Schwarzkopf, and G. Raithel, "Measurement of the van der Waals interaction by atom trajectory imaging," *Phys. Rev. A* **92**, 040701 (2015).
40. W. T. Liao, A. Pálffy, and C. H. Keitel, "Nuclear coherent population transfer with X-ray laser pulses," *Phys. Lett. B* **705**, 134–138 (2011).
41. A. Crespi, S. Longhi, and R. Osellame, "Photonic realization of the quantum Rabi model," *Phys. Rev. Lett.* **108**, 163601 (2012).
42. B. W. Adams, C. Butha, S. M. Cavalettob, J. Eversb, Z. Harmanbc, C. H. Keitelb, A. Pálffy, A. Picóna, R. Röhlsbergerd, Y. Rostovtseve, and K. Tamasakuf, "X-ray quantum optics," *J. Mod. Opt.* **60**, 2–21 (2013).

1. Introduction

Preparation and manipulation of a well-defined quantum state is of fundamental importance since it is extensively applied to many branches of physics ranging from laser physics [1] to quantum information processing [2].

In quantum information processing, using highly excited Rydberg states allows one to switch on and off strong interaction that are necessary for engineering many-body quantum states, towards implementing quantum simulation with large arrays of Rydberg atoms [3]. However, the transition frequency from Rydberg states to ground state falls generally in the ultraviolet region, which makes the transition difficult with a single laser. To complete the transition, two

lasers (two-photon processes) are required [4, 5]. The drawback by this method is that the transfer efficiency may not be high. This gives rise to a question that does the transition from the ground state to Rydberg states occur by lasers with frequency far-off-resonant with respect to the transition frequency?

Long-lived excited nuclear states (also known as isomers) can store large amounts of energy over longer periods of time. Release on demand of the energy stored in the metastable state called isomer depletion together with nuclear batteries [6–9], have received great attention in the last one and a half decades. Depletion occurs when the isomer is excited to a higher level, which is associated with freely radiating states and therefore releases the energy of the metastable state. Coherent population transfer between nuclear states would therefore not only be a powerful tool for preparation and detection in nuclear physics, but also especially useful for control of energy stored in isomers.

In atomic physics, a successful and robust technique for atomic coherent population transfer is the stimulated Raman adiabatic passage (STIRAP) [10]. The transfer of such techniques to nuclear systems, although encouraged by progress of laser technology, has not been accomplished due to the lack of γ -ray lasers.

To bridge the gap between X-ray laser frequency and nuclear transition energies, a key scheme is to combine moderately accelerated target nuclei and novel X-ray lasers [11]. Using this proposal, the interaction of X-rays from the European X-ray Free Electron Laser (XFEL) [12] with nuclear two-level systems was studied theoretically [11, 13]. However, the coherent control of isomers have never been addressed, partially because of the poor coherence properties of the XFEL. This raises again the question that whether the population transfer can be performed with high fidelity by off-resonant drivings. In this work, we present a proposal for population transfer between two states using lasers off-resonant with the transition energies of the two states. Note that there also exist several work [14–16] investigating population transfer by using only non-resonant driving fields recently, which can be explained by the superoscillation phenomenon. However, the major difference is that the driving fields is periodic in our work. In particular, we consider two types of pulse, i.e., square-well pulse and Gaussian pulse, as the driving fields.

2. Physical mechanism for population transfer

Consider a two-level system described by a Hamiltonian with general form ($\hbar = 1$)

$$H = \vec{d} \cdot \vec{\sigma} + \varepsilon \cdot \mathbb{1}, \quad (1)$$

where $\vec{d} = (d_x, d_y, d_z)$, and $\vec{\sigma} = (\sigma_x, \sigma_y, \sigma_z)$ represent Pauli matrices. $\mathbb{1}$ is the 2×2 identity matrix. This simple model can be employed to describe various physical systems ranging from natural microscopic system (e.g., atomic or spin system) to artificial mesoscopic system (e.g., superconducting circuits or semiconductor quantum dots). Since the identity matrix term adds an overall energy level shift to system, it only affects the global phase in dynamics evolution and can be ignored safely in later discussion. The evolution operator of this system then can be obtained after some straightforward algebras,

$$U(t, 0) = e^{-iHt} = \begin{pmatrix} P(t) - iQ(t) & -R(t)e^{-i(\theta - \frac{\pi}{2})} \\ R(t)e^{i(\theta - \frac{\pi}{2})} & P(t) + iQ(t) \end{pmatrix}, \quad (2)$$

where $P(t) = \cos(|\vec{d}|t)$, $Q(t) = \frac{d_z}{|\vec{d}|} \sin(|\vec{d}|t)$, $R(t) = \frac{\sqrt{d_x^2 + d_y^2}}{|\vec{d}|} \sin(|\vec{d}|t)$, $|\vec{d}| = \sqrt{d_x^2 + d_y^2 + d_z^2}$, and $\tan \theta = \frac{d_y}{d_x}$. When d_z is sufficiently large (i.e., $d_z \gg \sqrt{d_x^2 + d_y^2}$), $R(t) \simeq 0$. As a result, the transition between two levels will be sharply suppressed.

In this work we focus on the system dynamics driven by periodic square-well driving field. That is, the system is governed by the Hamiltonian $H_1 = \vec{d}_1 \cdot \vec{\sigma}$ in the time interval $[0, t_1]$, while the Hamiltonian is $H_2 = \vec{d}_2 \cdot \vec{\sigma}$ in the time interval $(t_1, T]$. T is the period of the square-well driving field, $t_2 = T - t_1$. The evolution operator within one period of time can be written as,

$$U(T, 0) = e^{-iH_2 t_2} e^{-iH_1 t_1} = \begin{pmatrix} \cos \phi & -\sin \phi e^{-i\theta} \\ \sin \phi e^{i\theta} & \cos \phi \end{pmatrix}, \quad (3)$$

where $\tan \phi = \frac{|\vec{v} \times \vec{d}_1 \times \vec{d}_2|}{\vec{d}_1 \cdot \vec{d}_2}$, $\vec{v} = (0, 0, 1)$, $\tan \theta = \frac{d_{1y}}{d_{1x}} = \frac{d_{2y}}{d_{2x}}$, and $|\vec{d}_1|t_1 = |\vec{d}_2|t_2 = \frac{\pi}{2} + 2m\pi$ (m is an arbitrary integer). For a periodic system, one can calculate the time-independent effective Hamiltonian from the evolution operator via definition $U(T, 0) \equiv e^{-iH_{eff}T}$ [17], and the effective Hamiltonian reads

$$H_{eff} = \frac{1}{T} \begin{pmatrix} 0 & \phi e^{-i(\theta + \frac{\pi}{2})} \\ \phi e^{i(\theta + \frac{\pi}{2})} & 0 \end{pmatrix}. \quad (4)$$

It is interesting to find that in the periodic driving field, the transition between two levels is determined by ϕ instead of the condition $d_z \gg \sqrt{d_x^2 + d_y^2}$ (it is called large detuning condition in atomic system). In other words, the periodic driving field can be viewed as the constant driving field with the effective coupling strength $\Lambda = \frac{\phi}{T} e^{-i(\theta + \frac{\pi}{2})}$ at the exact resonance condition. Although the effective coupling strength may be very small, it can still realize population transfer with the increasing of evolution time.

Note that, at an arbitrary time $t = t' + nT$ (n is the number of evolution periods), the evolution operator can be written as

$$U(t, 0) = \begin{cases} e^{-iH_1 t'} U(nT, 0), & t' \in [0, t_1], \\ e^{-iH_2(t' - t_1)} e^{-iH_1 t_1} U(nT, 0), & t' \in (t_1, T], \end{cases} \quad (5)$$

where the analytical expressions of $e^{-iH_1 t'}$ and $e^{-iH_2 t'}$ can be obtained from Eq.(2), and $U(nT, 0) = \vec{d}' \cdot \vec{\sigma} + \cos n\phi \cdot \mathbb{1}$, $\vec{d}' = (i \sin n\phi \sin \theta, -i \sin n\phi \cos \theta, 0)$. With this evolution operator $U(t, 0)$ we can know the state at arbitrary time in periodic driving system.

3. Examples

As an example, we show how to achieve population inversion $|0\rangle \rightarrow |1\rangle$ in a two-level atomic system to which a classical field is applied. The system Hamiltonian reads

$$H_0 = \omega_0 |1\rangle\langle 1| + \Omega e^{-i\omega_l t} |0\rangle\langle 1| + H.c., \quad (6)$$

where ω_0 and ω_l are the atomic transition frequency and laser frequency, respectively. Ω is the coupling constant. In the interaction picture, it becomes $H = \Delta |1\rangle\langle 1| + \Omega |0\rangle\langle 1| + H.c.$, where the detuning $\Delta = \omega_0 - \omega_l$. Comparing with Eq. (1) one obtains $\vec{d} = (\Omega, 0, \frac{\Delta}{2})$. Note that it is easy to control laser intensity to change the coupling constant and regulate laser frequency to change the detuning. Here we adopt two different ways to achieve population inversion, i.e., by manipulating the coupling constants Ω_1 and Ω_2 with a fixed large detuning Δ (called intensity modulation) or by manipulating the detunings Δ_1 and Δ_2 with a fixed coupling constant Ω (called frequency modulation). Figs. 1(a) and 1(b) demonstrate Rabi-like oscillations in dynamics evolution by periodic intensity and frequency modulations. For comparison we plot the dynamics evolution without periodic modulation in Fig. 1(c). Note that the frequency of the Rabi-like oscillation approximately equals to $|\Lambda|$ (see the dash lines in Fig. 1), which is in good agreement with the effective coupling strength of the effective Hamiltonian (4).

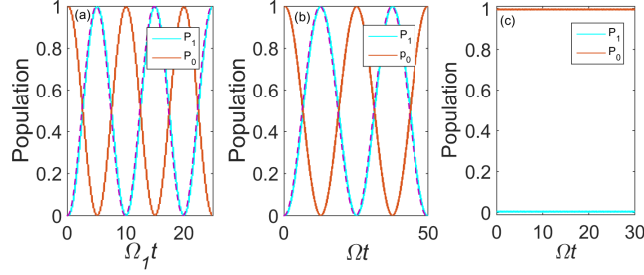


Fig. 1. The population as a function of time where P_0 (P_1) is the population of state $|0\rangle$ ($|1\rangle$). (a) The intensity modulation, $\Delta/\Omega_1 = 30$, $\Omega_2/\Omega_1 = 2$. (b) The frequency modulation, $\Delta_1/\Omega = 20$, $\Delta_2/\Omega = 30$. (c) The constant Rabi frequency and detuning, $\Delta_1/\Omega = 20$. The dash lines represent the function $|\sin \Lambda t|^2$.

The total time needed to achieve population inversion is,

$$\mathcal{T} = \frac{(4m+1)\pi^2(|\vec{d}_1| + |\vec{d}_2|)}{4\phi|\vec{d}_1||\vec{d}_2|}, \quad m = 0, 1, 2, \dots \quad (7)$$

As shown in Eq.(7), the minimal time \mathcal{T}_f ($m = 0$) is determined by both the coupling constants and the detunings. This gives rise to a question whether there exists a set of parameters $\{\Omega_j, \Delta_j\}$ to make \mathcal{T}_f minimum. By expanding Eq.(7) up to the first order in ϕ (i.e., $\tan \phi \sim \phi$), it is not hard to find that $\mathcal{T}_f \simeq \frac{\pi^2}{4} \frac{\Delta_1 + \Delta_2}{|\Delta_1 \Omega_2 - \Delta_2 \Omega_1|}$. Obviously, in the intensity modulation, the minimal time \mathcal{T}_f becomes short when the difference between two coupling constants is great. When the coupling constant Ω_1 approaches the coupling constant Ω_2 , the minimal time \mathcal{T}_f approaches infinity. This is not surprise since the system in this situation returns to the case of constant driving with large detuning, and the dynamics is frozen when $\Omega_1 = \Omega_2$. In the frequency modulation, the main results are similar to those of the intensity modulation. The difference is that the minimal time \mathcal{T}_f almost remains unchanged when only one of the detunings varies, and it

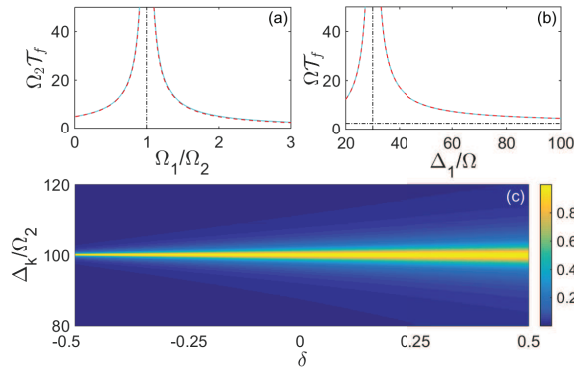


Fig. 2. The minimal time \mathcal{T}_f as a function of (a) the coupling constant Ω_1 in the intensity modulation, $\Delta/\Omega_2 = 30$; (b) the detuning Δ_1 in the frequency modulation, $\Delta_2/\Omega = 30$. The solid and dash lines are the exact and approximate results, respectively. The horizontal line (dot-dash line) is for $\mathcal{T}_f' = \frac{\pi^2}{4\Omega}$. (c) The population with different detunings Δ_k in the intensity modulation, where the square-well pulse is described by $\Omega_1/\Omega_2 = 3$ and $\Delta_1/\Omega_2 = 100$ for the transition $|0\rangle \leftrightarrow |1\rangle$.

asymptotically approaches $\frac{\pi^2}{4\Omega}$. Those observations can be verified by numerical calculations, as shown in Figs. 2(a) and 2(b). We can find that the first-order approximation is good enough to describe the total time \mathcal{T} in this case.

4. Robustness of the scheme and its extension to three-level systems

For a two-level system, the detuning (labelled as Δ_1) might be different from that used in the calculation. One then asks whether this mismatch affects population inversion in this scheme. In Fig. 2(c), we plot the population on the levels other than the target, where the detunings of these levels to the level $|0\rangle$ are denoted by Δ_k . We find in Fig. 2(c) that the effect is remarkable. E.g., the population is less than 0.1 when the detunings have 5% deviation from the detuning Δ_1 . Fig. 2(c) also shows that deviations in coupling constants Ω_1 [the deviation in the coupling constant is defined as $\Omega'_1 = (1 + \delta)\Omega_1$] has small influence on the population inversion $|0\rangle \rightarrow |1\rangle$.

Note that it may be difficult to obtain a perfect square-well field in practice. Thus we should analyze how deviations of the applied field from the perfect square-well one affect the population transfer. Taking the intensity modulation as an example, we replace the perfect square-well field with an approximate square-well field to study this effect. Assume that the approximate square-well field takes

$$\Omega(t) = \begin{cases} \Omega_2 + \frac{\Omega_1 - \Omega_2}{1 + e^{\gamma(t - \frac{T}{2})}}, & t < 0.5t_1, \\ \Omega_2 + \frac{\Omega_1 - \Omega_2}{1 + e^{-\gamma(t - T + \frac{T}{2})}}, & t \geq 0.5t_1, \end{cases} \quad (8)$$

where $t_1 = \frac{\pi}{2|\Delta_1|}$. We adopt a convention that $t = (t \bmod T)$ if $t > T$, and the parameter $\gamma > 0$ is used to adjust the hardness of the square-well field. Apparently, the larger γ is, the harder the square-well field would be. When $\gamma \rightarrow +\infty$, this expression approaches to the perfect square-well field. In Fig. 3 we plot the population P_1 when the square-well field is not perfect. For small deformation of the square-well field (i.e., γ is not very small), it does not have obvious influences on the system dynamics [cf. Figs. 3(a) and 3(b)]. Interestingly, even the square-well field approximately takes a triangular shape, as shown in Fig. 3(d), population transfer can also be realized, but the total time to reach population inversion has been changed.

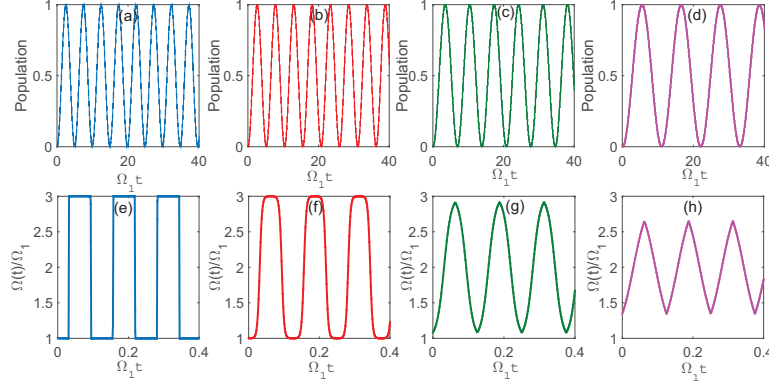


Fig. 3. The population P_1 as a function of time with different γ in the intensity modulation. (a) $\gamma = 10000$. (b) $\gamma = 300$. (c) $\gamma = 100$. (d) $\gamma = 50$. The bottom panels (e)-(h) are the square-well field corresponding to the top panels (a)-(d), respectively. The parameters of perfect square-well field are $\Omega_2/\Omega_1 = 3$ and $\Delta/\Omega_1 = 50$.

In actual modulation, there might exist errors such as perturbations or noises in the coupling constant or the detuning. Taking the intensity modulation as an example again, we add noise

terms $\varepsilon(t)$ into the perfect square-well field, which are taken randomly in a certain interval. The results are plotted in Fig. 4, which suggests that the system dynamics is robust against noises.

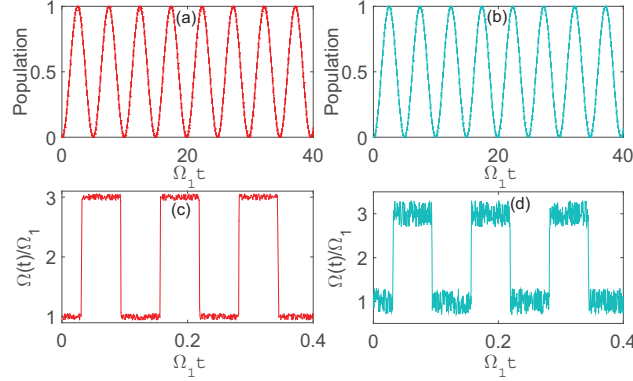


Fig. 4. The population P_1 as a function of time with noisy square-well field. (a) The noise $\varepsilon(t)$ is generated randomly in the interval $[-0.05, 0.05]$. (b) The noise $\varepsilon(t)$ is generated randomly in the interval $[-0.3, 0.3]$. The bottom panels (c) and (d) are the noisy square-well fields corresponding to the top panels (a) and (b), respectively. For perfect square-well fields, we employ $\Omega_2/\Omega_1 = 3$, and $\Delta/\Omega_1 = 50$ in the intensity modulation.

So far, we do not consider the effect of environment yet. In the presence of decoherence, we can use the following master equation to describe the system dynamics [18],

$$\dot{\rho}(t) = -i[H(t), \rho(t)] + \mathcal{L}_{01}(\rho) + \mathcal{L}_{11}(\rho), \quad (9)$$

where $\mathcal{L}_{01}(\rho) = \frac{\gamma_{01}}{2}(2\sigma_{01}\rho\sigma_{10} - \sigma_{10}\sigma_{01}\rho - \rho\sigma_{10}\sigma_{01})$ and $\mathcal{L}_{11}(\rho) = \frac{\gamma_{11}}{2}(2\sigma_{11}\rho\sigma_{11} - \sigma_{11}\sigma_{11}\rho - \rho\sigma_{11}\sigma_{11})$. Here, γ_{01} and γ_{11} are the dissipation and the dephasing rate, respectively. $\sigma_{ij} = |i\rangle\langle j|$ for $i, j \in \{0, 1\}$. Fig. 5 shows the population of state $|1\rangle$ versus the dissipation and dephasing rates. We find that the population transfer suffers from the dissipation rate much more than the dephasing rate.

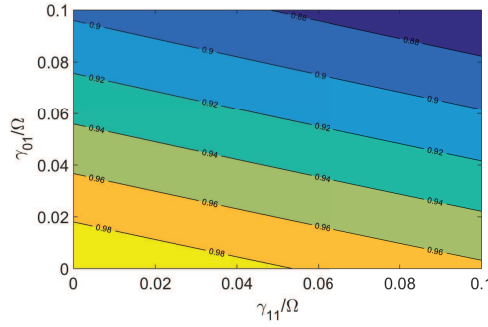


Fig. 5. The population versus the dissipation rate γ_{01} and the dephasing rate γ_{11} . The initial state is $|0\rangle$, $\Delta_1/\Omega = 30$, $\Delta_2/\Omega = 300$.

Next we study the situation that the detuning is not very large. That is, in the intensity manipulation, one of coupling constants (say, Ω_1) is not very small compared to the detuning. If the system parameters satisfy one of the following equations,

$$d_{1x}\sin(m\phi) + d_{1z}\cos(m\phi) = |\vec{d}_1|, \quad m = 1, 2, 3, \dots, \quad (10)$$

the system would stay in the target state for a long time with respect to the case without this condition, as shown in Fig. 6(b). One can observe plateaus in the time evolution when the population reaches one. Those plateaus provide us with large opportunity to stop the population transfer, and make the system stay at the high level forever. Physically this originates from the small coupling constant (such as Ω_2) while another is very large. In this case, the system is shortly frozen when it arrives at one of the two levels.

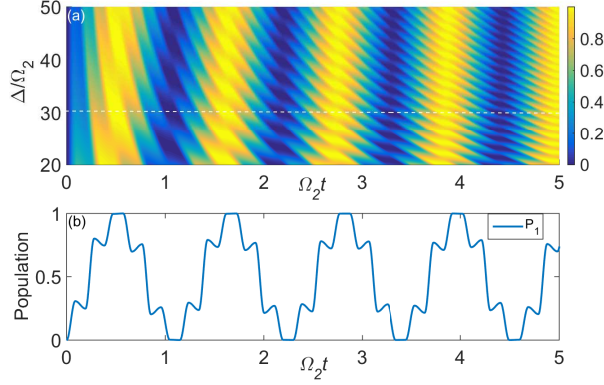


Fig. 6. (a) The population as a function of time and detuning, $\Omega_1/\Omega_2 = 10$. (b) The population as a function of time when $\Delta/\Omega_2 = 30$ (the dash line), where the parameters approximately satisfy Eq.(10).

This technique can be extended to achieve an arbitrary coherent superposition state, for example, $|\Psi_T\rangle = \cos\Theta|0\rangle + \sin\Theta|1\rangle$ in the Λ -type (or V -type) three-level system, where two lower levels couple to another through classical fields with coupling constant Ω_1 and Ω_2 , respectively. Both detunings are assumed to be the same Δ . At first, we should choose the ratio of Ω_1/Ω_2 to equal $\tan(\Theta)$ given in $|\Psi_T\rangle$. By periodically changing the detunings Δ_a and Δ_b with fixed coupling constant Ω_1 and Ω_2 , one can achieve the state $|\Psi_T\rangle$. If the three-level atom is placed in a cavity, and one of the transition is driven by the cavity field while the other is driven by a classical field, we can realize single photon storing by manipulating the frequency and the intensity of the classical field (for details, see Appendix).

In experiments, the coupling might not be a constant for laser pulse drivings. Further investigation shows that the scheme works well provided that the pulse takes a Gaussian form $\Omega(t) = \mathcal{A} e^{-\frac{(t-4\xi)^2}{2\xi^2}}$. Here \mathcal{A} and ξ denote the amplitude and the width of the Gaussian pulse, respectively. In this case the period T is the time width of full Gaussian pulse, and we truncate the width of Gaussian pulse with $T = 8\xi$ in the following. The evolution operator can be written as $U(T, 0) = \mathbb{T} e^{-i \int_0^T H(t') dt'}$ with \mathbb{T} denoting the time-ordering operator. It is difficult to find an analytical expression for the evolution operator. Fortunately, we can prove that after n Gaussian pulses the system evolution operator takes following form

$$U(nT, 0) = \begin{pmatrix} \cos(n\vartheta) - i \frac{Q' \sin(n\vartheta)}{\sqrt{Q'^2 + R'^2}} & -\frac{R'}{\sqrt{Q'^2 + R'^2}} \sin(n\vartheta) e^{i\theta'} \\ \frac{R'}{\sqrt{Q'^2 + R'^2}} \sin(n\vartheta) e^{-i\theta'} & \cos(n\vartheta) + i \frac{Q' \sin(n\vartheta)}{\sqrt{Q'^2 + R'^2}} \end{pmatrix}.$$

where $\cos \vartheta = P'$ and the constants $\{P', Q', R', \theta'\}$ are jointly determined by \mathcal{A} , ξ , and Δ . One easily observes that if $Q' \neq 0$, namely there exists an imaginary part in the evolution operator $U(T, 0)$, the population inversion cannot be perfectly obtained. We can adjust the parameters $\{\mathcal{A}, \xi, \Delta\}$ to make Q' vanish and approximately realize population inverse after N Gaussian

pulses with $N = \frac{(4m+1)\pi}{2\eta}$, $m = 0, 1, 2, \dots$. Fig. 7 demonstrates how the parameters $\{\mathcal{A}, \xi, \Delta\}$ of the Gaussian pulse affects the system dynamics. It indicates that we can still achieve population inversion with appropriate Gaussian pulses even though the system is driven by lasers off-resonant with the transition energy.

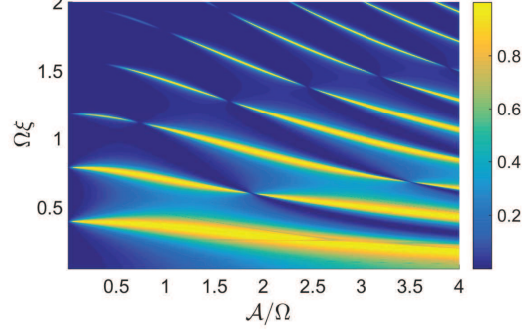


Fig. 7. The population versus $\{\mathcal{A}, \xi\}$ of the Gaussian pulse, $\Delta/\Omega = 2$.

5. Extension to Rabi model

The Rabi model [19–23] describes a two-level atom (system) coupled to a single-mode electromagnetic field, which provides us with a simplest example for light-matter interactions. The Hamiltonian describing such a system reads

$$H = \omega_b a^\dagger a + \frac{\omega_0}{2} \sigma_z + \Omega \sigma_x (a^\dagger + a), \quad (11)$$

where σ_x and σ_z are Pauli matrices for the two-level system with level splitting ω_0 . a (a^\dagger) is the annihilation (creation) operator of the single mode field with frequency ω_b . Ω denotes the coupling constant between the two-level system and the field. Note that the Hamiltonian (11) describes the simplest interaction between atom and field, and can be solved analytically [24, 25]. Rewriting the Hamiltonian (11) in the Hilbert space spanned by $\{|g, 0\rangle, |e, 0\rangle, |g, 1\rangle, |e, 1\rangle, \dots, |g, n\rangle, |e, n\rangle, \dots\}$, where $|f, n\rangle$ denotes the state that the two-level system in state $|f\rangle$ ($f = e, g$) with n photons in the field, we have

$$H = \begin{pmatrix} -\frac{\omega_0}{2} & 0 & 0 & \Omega & 0 & 0 & 0 & \dots \\ 0 & \frac{\omega_0}{2} & \Omega & 0 & 0 & 0 & 0 & \dots \\ 0 & \Omega & -\frac{\omega_0}{2} + \omega_b & 0 & 0 & \Omega & 0 & \dots \\ \Omega & 0 & 0 & \frac{\omega_0}{2} + \omega_b & \Omega & 0 & 0 & \dots \\ 0 & 0 & 0 & \Omega & -\frac{\omega_0}{2} + 2\omega_b & 0 & 0 & \dots \\ 0 & 0 & \Omega & 0 & 0 & \frac{\omega_0}{2} + 2\omega_b & \Omega & \dots \\ 0 & 0 & 0 & 0 & 0 & \Omega & -\frac{\omega_0}{2} + 3\omega_b & \dots \\ \vdots & \vdots & \vdots & \vdots & \vdots & \vdots & \vdots & \ddots \end{pmatrix}. \quad (12)$$

Then the system dynamics is governed by Liouville equation

$$\dot{\rho}(t) = -i[H, \rho(t)], \quad (13)$$

where $\rho(t)$ is the density operator for the composite system (atom plus field).

Suppose the two-level system is in the ground state $\rho^s(0) = |g\rangle\langle g|$ and the field is in a coherent state initially, namely

$$\rho_{nn}^b(0) = \frac{\langle n \rangle^n e^{-\langle n \rangle}}{n!}. \quad (14)$$

We find that it is still unavailable to realize population inversion perfectly starting from $\rho(0) = \rho^s(0) \otimes \rho^b(0)$ by the constant driving field, even though the transition frequency of the two-level system is on resonance with the frequency of field (i.e., $\Delta = \omega_0 - \omega_b = 0$), as shown in Fig. 8(a). This is quite different from the Jaynes-Cummings (JC) model [26] where it is applied the rotation-wave approximation to this model. Physically, this result originates from the emergence of counter-rotating part, i.e., $\sigma^+ a^\dagger$ and $\sigma^- a$ in Hamiltonian (11), where σ^+ (σ^-) is the raising (lowering) operator for the two-level system. From the aspect of the field, it does not remain coherent state any more, as shown in Fig. 8(b).

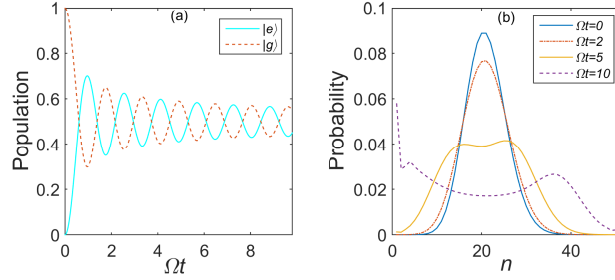


Fig. 8. (a) The population of $|e\rangle$ and $|g\rangle$ as a function of time with resonant atom-field couplings (i.e., $\Delta = \omega_0 - \omega_b = 0$). (b) The probability that there are n photons in the field at different time. The field is initially in a coherent state given by Eq.(14) with the average photon number $\langle n \rangle = 20$. The photon number is truncated at 51 in numerical calculations.

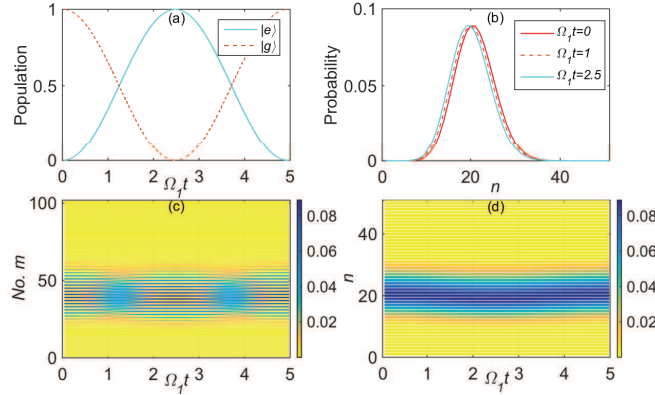


Fig. 9. (a) The population of $|e\rangle$ and $|g\rangle$ as a function of time in the intensity modulation, $\Delta/\Omega_1 = 300$, $\Omega_2/\Omega_1 = 3$. (b) The probability that there are n photons in the field at different time. The field is initially in a coherent state described by Eq.(14) with $\langle n \rangle = 20$. (c) The occupation of No. m basis as a function of time, where the basis are ordered as $\{|g, 0\rangle, |e, 0\rangle, |g, 1\rangle, |e, 1\rangle, \dots, |g, 50\rangle, |e, 50\rangle, |g, 51\rangle\}$. (d) The probability of n photons in the field as a function of time.

In contrast, by the intensity modulation, we can realize the population transfer as shown in the following. Keeping the detuning ($\Delta = \omega_b - \omega_0$) fixed, and modulating the coupling constant

Ω_1 and Ω_2 , we plot the evolution of the population in Fig. 9(a). We find that population transfer from $|g\rangle$ to $|e\rangle$ occurs at $\Omega_1 t = 2.5$. An inspection of Fig. 9(b) shows that the state of the field (the coherent state) remains unchanged in the dynamics [see Fig. 9(d) as well]. Furthermore, we find that population transfer can occur for a wide range of initial states of the field, as shown in Fig. 10, where the initial state of the field is $\rho_{nn}^b(0) = \mathcal{P}_n$. Here \mathcal{P}_n are a set of random numbers in interval $[0, 1]$ and satisfy the normalization condition $\sum_n \mathcal{P}_n = 1$.

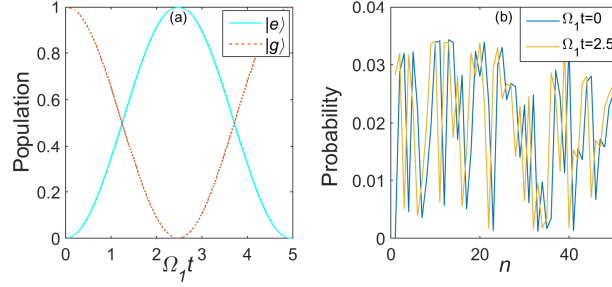


Fig. 10. (a) The population at $|e\rangle$ and $|g\rangle$ as a function of time in the intensity modulation. (b) The probability that there are n photons in the field at different time. The field is in random state initially.

6. Discussion and conclusion

On the other hand, this method can be applied to study Landau-Zener-Stückelberg interference [27–31], which has been observed in a superconducting qubit under periodic modulation [32–38]. Obviously, the Landau-Zener transition can also be fore-sight by using our method. In addition, the scheme can be used to realize population inversion for Rydberg states, e.g., from the ground state $|g\rangle \equiv 5S_{1/2}|F=2, m=2\rangle$ to the Rydberg state $|r\rangle \equiv 60S_{1/2}$ of the cold ^{87}Rb atom. Since this atomic transition frequency is in the ultraviolet region, it conventionally employs 780-nm and 480-nm lasers via the intermediate state $|e\rangle \equiv 5P_{3/2}|F=3, m=3\rangle$ under two-photon resonance condition [39]. In our scheme, only 780-nm lasers can work. The detuning between atomic transition frequency and 780-nm laser frequency is about $\Delta = 6.25 \times 10^8$ MHz, which is in the far-off-resonant regime. The two coupling strengths we employ are $\Omega_1 = 2\pi \times 30$ MHz and $\Omega_2 = 2\pi \times 300$ MHz. We can set $t_1 \simeq t_2 \simeq 5.03$ ps, and the addressing period $T \simeq 10.06$ ps. Note that the period of driving field should be modulated with high precision in the far-off-resonant regime. As a result the total time of realizing this transition is about $2.9 \mu\text{s}$.

The other possible application is to achieve long-lived excited nuclear states. The transition energy between the nuclear states is much larger than the energy of X-ray lasers. To compensate the energy difference between nuclear transition and X-ray laser, one envisages accelerated nuclei interacting with x-ray laser pulses. In the strong acceleration regime, the resonance condition cannot be satisfied very well for requiring high degree of accuracy of relativistic factor [11, 40]. As a result it significantly influences population transfer. Our calculations shows that this problem can be effectively solved by a series of Gaussian pulses. Take the E1 transition in ^{223}Ra as an example. It is impossible to transfer the population to excited state with only a single pulse when the detuning Δ is about 0.1 eV [11]. However, if we take a laser intensity $I = 9 \times 10^{22} \text{ W/cm}^2$ and the width of Gaussian pulse is 31 fs, the transition can be obtained by 5 Gaussian pulses.

In conclusion, a scheme to realize population transfer by far-off-resonant drivings is proposed. By two sequentially applied lasers with different frequency or intensity, population

transfer can be perfectly achieved in two-level systems. This proposal can be extended to N -level systems and to the case with cavity fields instead of classical fields. Furthermore, it can be exploited to achieve population transfer in the Rabi model regardless the form of bosonic field, which has been experimentally explored in the photonic analog simulator [41].

The scheme can be applied to population transfer from ground state to Rydberg states or Rydberg state preparation. In X-ray quantum optics [42], it may also find applications, since the lack of γ -ray lasers and huge transition energy inside the nuclei. This scheme can work with both square-well pulse and Gaussian pulse, and it is robust against dissipation and dephasing in the sense that the life-time of Rydberg states as well as the nuclear excited state is long. By manipulating the system parameters, we can make the system stay at the excited level longer. This work paves a new avenue in preparation and manipulation of quantum states with off-resonant driving fields, and might find potential applications in the field of quantum optics.

Appendix: Three-level system in periodic square-well fields

We now demonstrate how to apply the periodic modulation to the other structure of quantum systems—three-level system. As shown in Fig. 11(a), we consider a Λ -type three-level system (it also works in V -type system) that two levels coupled to the third with coupling constants Ω_1 and Ω_2 , respectively. Δ denotes the detuning in this system. Without loss of generality, we assume Ω_1 and Ω_2 to be real. In the interaction picture, the Hamiltonian in the Hilbert space spanned by $\{|0\rangle, |1\rangle, |2\rangle\}$ reads

$$H = \begin{pmatrix} 0 & 0 & \Omega_1 \\ 0 & 0 & \Omega_2 \\ \Omega_1 & \Omega_2 & \Delta \end{pmatrix}. \quad (15)$$

The evolution operator becomes

$$U(t, 0) = e^{-iHt} = e^{-\frac{i\Delta t}{2}} \begin{pmatrix} B_1 & B_2 & B_4 \\ B_2 & B_3 & B_5 \\ B_4 & B_5 & B_6 \end{pmatrix}, \quad (16)$$

where $B_1 = \frac{\Omega_2^2}{\Omega_1^2 + \Omega_2^2} e^{\frac{i}{2}\Delta t} + \frac{\Omega_1^2}{\Omega_1^2 + \Omega_2^2} (\cos \frac{y}{2} + i \frac{\Delta}{y} \sin \frac{y}{2})$, $B_2 = -\frac{\Omega_1 \Omega_2}{\Omega_1^2 + \Omega_2^2} e^{\frac{i}{2}\Delta t} + \frac{\Omega_1 \Omega_2}{\Omega_1^2 + \Omega_2^2} (\cos \frac{y}{2} + i \frac{\Delta}{y} \sin \frac{y}{2})$, $B_3 = \frac{\Omega_1^2}{\Omega_1^2 + \Omega_2^2} e^{\frac{i}{2}\Delta t} + \frac{\Omega_2^2}{\Omega_1^2 + \Omega_2^2} (\cos \frac{y}{2} + i \frac{\Delta}{y} \sin \frac{y}{2})$, $B_4 = -2i \frac{\Omega_1}{y} \sin \frac{y}{2}$, $B_5 = -2i \frac{\Omega_2}{y} \sin \frac{y}{2}$, $B_6 = \cos \frac{y}{2} - i \frac{\Delta}{y} \sin \frac{y}{2}$, and $y = \sqrt{4\Omega_1^2 + 4\Omega_2^2 + \Delta^2}$. When the initial state is $|2\rangle$ and in the large detuning limit (i.e., $\Delta \gg \Omega_1, \Omega_2$), we find that $B_4 \simeq B_5 \simeq 0$ in the evolution operator. Thus the population transfer can not be realized in this case.

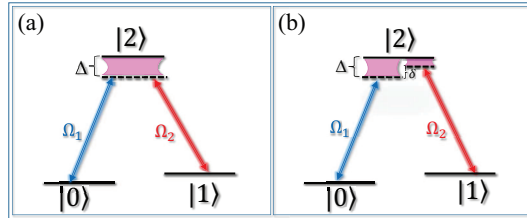


Fig. 11. The level configuration of a three-level system.

Now we turn to study the system dynamics under periodic frequency modulation. That is, the Hamiltonian is H_a in the time interval $[0, t_1]$ and H_b in the time interval $(t_1, T]$, where

$H_j = \begin{pmatrix} 0 & 0 & \Omega_1 \\ 0 & 0 & \Omega_2 \\ \Omega_1 & \Omega_2 & \Delta_j \end{pmatrix}$, $j = a, b$. Note that both Δ_a and Δ_b are chosen to be very large, so the system dynamics is frozen with only a single driving. The evolution operator of one period can be calculated as

$$U(T, 0) = e^{-iH_b t_2} e^{-iH_a t_1} = \frac{e^{-\frac{i}{2}(\Delta_a t_1 + \Delta_b t_2)}}{y_a y_b} \begin{pmatrix} B'_1 & B'_2 & B'_4 \\ B'_2 & B'_3 & B'_5 \\ -B'_4 & -B'_5 & B'_6 \end{pmatrix}, \quad (17)$$

where $B'_1 = \frac{1}{\Omega_1^2 + \Omega_2^2} [y_a y_b \Omega_2^2 e^{\frac{i}{2}(\Delta_a t_1 + \Delta_b t_2)} - \Omega_1^2 (4\Omega_1^2 + 4\Omega_2^2 + \Delta_a \Delta_b)]$, $B'_2 = -\frac{1}{\Omega_1^2 + \Omega_2^2} [y_a y_b \Omega_1 \Omega_2 e^{\frac{i}{2}(\Delta_a t_1 + \Delta_b t_2)} + \Omega_1 \Omega_2 (4\Omega_1^2 + 4\Omega_2^2 + \Delta_a \Delta_b)]$, $B'_3 = \frac{1}{\Omega_1^2 + \Omega_2^2} [y_a y_b \Omega_1^2 e^{\frac{i}{2}(\Delta_a t_1 + \Delta_b t_2)} - \Omega_2^2 (4\Omega_1^2 + 4\Omega_2^2 + \Delta_a \Delta_b)]$, $B'_4 = 2\Omega_1 (\Delta_b - \Delta_a)$, $B'_5 = 2\Omega_2 (\Delta_b - \Delta_a)$, and $B'_6 = -4(\Omega_1^2 + \Omega_2^2) - \Delta_a \Delta_b$. We have set $y_a t_1 = y_b t_2 = \pi$, $y_j = \sqrt{4\Omega_1^2 + 4\Omega_2^2 + \Delta_j^2}$, $j = a, b$. Since the evolution operator is time-dependent, it is difficult to calculate the system dynamics analytically for n evolution periods. Further observations demonstrate that if the system state $|\Psi(t)\rangle = c_0(t)|0\rangle + c_1(t)|1\rangle + c_2(t)|2\rangle$ satisfies the condition $\frac{c_0(t)}{c_1(t)} = \frac{\Omega_1}{\Omega_2}$, the evolution operator would be time-independent. Then the evolution operator after n evolution periods becomes

$$U(t, 0) = U(nT, 0) = \frac{e^{-\frac{i\pi}{2}(\Delta_a t_1 + \Delta_b t_2)}}{(y_a y_b)^n} \begin{pmatrix} \frac{\Omega_1^2}{2(\Omega_1^2 + \Omega_2^2)}(s_1^n + s_2^n) & \frac{\Omega_1 \Omega_2}{2(\Omega_1^2 + \Omega_2^2)}(s_1^n + s_2^n) & \frac{i\Omega_1}{2\sqrt{\Omega_1^2 + \Omega_2^2}}(s_1^n - s_2^n) \\ \frac{\Omega_1 \Omega_2}{2(\Omega_1^2 + \Omega_2^2)}(s_1^n + s_2^n) & \frac{\Omega_2^2}{2(\Omega_1^2 + \Omega_2^2)}(s_1^n + s_2^n) & \frac{i\Omega_2}{2\sqrt{\Omega_1^2 + \Omega_2^2}}(s_1^n - s_2^n) \\ \frac{-i\Omega_1}{2\sqrt{\Omega_1^2 + \Omega_2^2}}(s_1^n - s_2^n) & \frac{-i\Omega_2}{2\sqrt{\Omega_1^2 + \Omega_2^2}}(s_1^n - s_2^n) & \frac{1}{2}(s_1^n + s_2^n) \end{pmatrix},$$

where $s_1 = d_1 + id_2 = |s|e^{i\varphi}$, $s_2 = d_1 - id_2 = |s|e^{-i\varphi}$, $\tan \varphi = \frac{d_2}{d_1}$, $|s| = \sqrt{d_1^2 + d_2^2}$, $d_1 = -4\Omega_1^2 - 4\Omega_2^2 - \Delta_a \Delta_b$, and $d_2 = 2(\Delta_a - \Delta_b)\sqrt{\Omega_1^2 + \Omega_2^2}$. When the initial state is $|\Psi(0)\rangle = |2\rangle$, the final state becomes

$$|\Psi(t)\rangle = U(nT, 0)|\Psi(0)\rangle = \mathcal{N} \begin{pmatrix} \Omega_1 \sin(n\varphi) \\ \Omega_2 \sin(n\varphi) \\ -i\sqrt{\Omega_1^2 + \Omega_2^2} \cos(n\varphi) \end{pmatrix}, \quad (18)$$

where \mathcal{N} is a normalization constant. Note that whether the system evolves or not depends only on the phase φ , regardless of the large detuning condition, and the Rabi-like oscillation frequency is determined by the phase φ .

We next demonstrate how to realize an arbitrary coherent superposition state $|\Psi_T\rangle = \cos\Theta|0\rangle + \sin\Theta|1\rangle$ in the Λ -type (or V -type) three-level system. We regulate the detunings Δ_a and Δ_b and fix the coupling constants Ω_1 and Ω_2 . Especially, the ratio of Ω_1/Ω_2 is modulated to equal $\tan\Theta$ in $|\Psi_T\rangle$. Again, we study in the large detuning regime. According to Eq.(18), if we set $N\varphi = \frac{\pi}{2}$, the system would arrive at the coherent superposition state $|\Psi_T\rangle$ and the total time of achieving $|\Psi_T\rangle$ is about

$$\mathcal{T} = \frac{\pi}{2 \tan^{-1} \left| \frac{2(\Delta_a - \Delta_b)\sqrt{\Omega_1^2 + \Omega_2^2}}{4\Omega_1^2 + 4\Omega_2^2 + \Delta_a \Delta_b} \right|} \left(\frac{\pi}{\sqrt{4\Omega_1^2 + 4\Omega_2^2 + \Delta_a^2}} + \frac{\pi}{\sqrt{4\Omega_1^2 + 4\Omega_2^2 + \Delta_b^2}} \right). \quad (19)$$

For comparison, we plot the system dynamics under constant driving field with the detuning $\Delta/\Omega_1 = 50$ in Fig. 12(a) and $\Delta/\Omega_1 = 100$ in Fig. 12(b), where the fixed coupling constants

satisfy $\Omega_2/\Omega_1 = 2$. One can find that the system dynamics is frozen due to the large detuning condition. However, as shown in Fig. 12(c), it is completely different in the frequency modulation, where two tunable detunings are also $\Delta_a/\Omega_1 = 50$ and $\Delta_b/\Omega_1 = 100$. Namely, the population transfer can be realized in the later case.

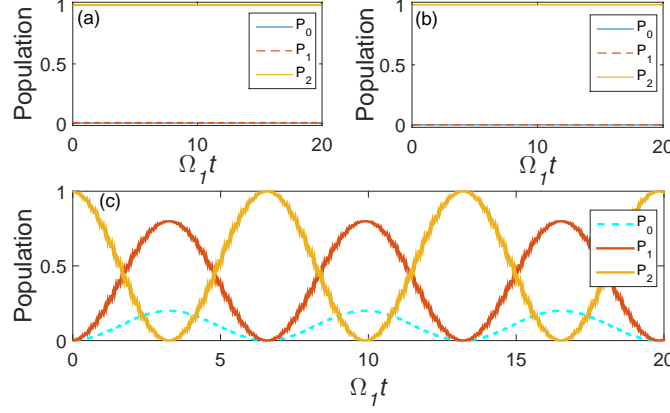


Fig. 12. The population as a function of time where the initial state is $|2\rangle$. (a) $\Delta/\Omega_1 = 50$, $\Omega_2/\Omega_1 = 2$. (b) $\Delta/\Omega_1 = 100$, $\Omega_2/\Omega_1 = 2$. (c) $\Delta_a/\Omega_1 = 50$, $\Delta_b/\Omega_1 = 100$, $\Omega_2/\Omega_1 = 2$.

Note that our theory can also be generalized into N -level systems, where one level couples to the reminder levels with the corresponding coupling constants $\Omega_1, \Omega_2, \dots, \Omega_N$, and all the detunings are Δ . By a similar procedure shown above in the frequency modulation, we can obtain the following coherent superposition state,

$$|\Psi_T\rangle = \mathcal{N}(\Omega_1|0\rangle + \Omega_2|1\rangle + \dots + \Omega_N|N-1\rangle), \quad (20)$$

where the coefficients $\Omega_1, \Omega_2, \dots, \Omega_N$ are determined by coupling constants and \mathcal{N} is a normalization constant.

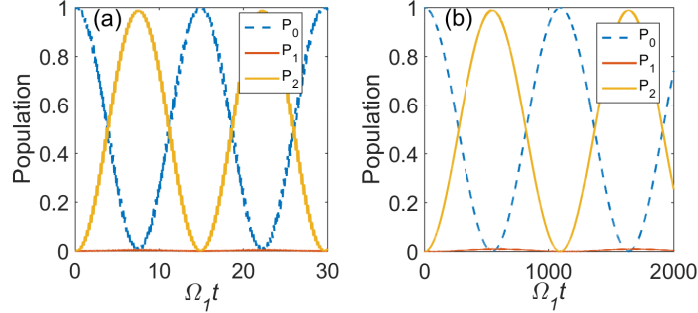


Fig. 13. The population as a function of time in frequency modulation. The initial state is $|0\rangle$. (a) $\Delta_\alpha/\Omega_1 = 40$, $\Delta_\beta/\Omega_1 = 20$, $\delta/\Omega_1 = 10$, $\Omega_2 = \Omega_1$. (b) $\delta_\alpha = 0$, $\delta_\beta/\Omega_1 = 30$, $\Delta/\Omega_1 = 10$, $\Omega_2/\Omega_1 = \Omega_1$.

Next, we show how to modulate the detunings Δ or δ to realize population transfer $|0\rangle \rightarrow |2\rangle$ in Fig. 11(b). Numerical simulation results are presented in Fig. 13. We regulate two detunings

Δ_α and Δ_β in Fig. 13(a), where two Hamiltonians read $H_j = \begin{pmatrix} 0 & 0 & \Omega_1 \\ 0 & \delta & \Omega_2 \\ \Omega_1 & \Omega_2 & \Delta_j \end{pmatrix}$, $j = \alpha, \beta$.

Fig. 13(b) demonstrates the dynamics by regulating two detunings δ_α and δ_β , where two Hamiltonians read $H_j = \begin{pmatrix} 0 & 0 & \Omega_1 \\ 0 & \delta_j & \Omega_2 \\ \Omega_1 & \Omega_2 & \Delta \end{pmatrix}$, $j = \alpha, \beta$. It is shown that the system evolves with time in both modulations, and one can obtain population transfer $|0\rangle \rightarrow |2\rangle$ by choosing the evolution time \mathcal{T} .

We should emphasize that the population transfer $|2\rangle \rightarrow |1\rangle$ can also be realized by intensity modulation. That is, the Hamiltonian is $H'_1 = \begin{pmatrix} 0 & 0 & \Omega_1 \\ 0 & \delta & \Omega_2 \\ \Omega_1 & \Omega_2 & \Delta \end{pmatrix}$ in the time interval $[0, t_1]$,

while the Hamiltonian is $H'_2 = \begin{pmatrix} 0 & 0 & \Omega_1 \\ 0 & \delta & \Omega'_2 \\ \Omega_1 & \Omega'_2 & \Delta \end{pmatrix}$ in the time interval $(t_1, T]$. The results are

plotted in Fig. 14. If we put the three-level atom in a cavity, the transition between $|0\rangle \leftrightarrow |2\rangle$ is coupled by the cavity field with the detuning Δ , and the transition between $|1\rangle \leftrightarrow |2\rangle$ is coupled by classical field with the detuning $\Delta - \delta$. The Hilbert space of the atom-cavity system is spanned by $\{|0, 1\rangle, |2, 0\rangle, |1, 0\rangle\}$, where $|m, n\rangle$ denotes the atom state $|m\rangle$ and n photons in the cavity. For the initial state $|0, 1\rangle$, by combining the frequency and intensity modulation of classical field to reach the state $|1, 0\rangle$, one can use it to realize single photon storing or releasing.

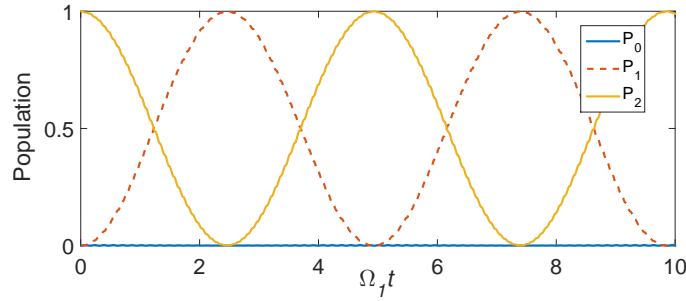


Fig. 14. The population as a function of time in intensity modulation. The initial state is $|2\rangle$, $\Delta/\Omega_1 = 40$, $\delta = 0$, $\Omega_2 = \Omega_1$, $\Omega'_2/\Omega_1 = -1$.

Acknowledgments

We thank Y. M. Liu for helpful discussions. This work is supported by the National Natural Science Foundation of China (NSFC) under Grants No.11534002 and No.61475033.

